Pharm Res (2014) 31:3445–3460
DOI 10.1007/s11095-014-1433-0

RESEARCH PAPER

siRNA-Mediated Knockdown of P450 Oxidoreductase in Rats: A Tool to Reduce Metabolism by CYPs and Increase Exposure of High Clearance Compounds

Rob S. Burke • Inthirai Somasuntharam • Paul Rearden • Duncan Brown • Sujal V. Deshmukh • Martha A. DiPietro • Jillian DiMuzio • Roy Eisenhandler • Scott E. Fauty • Christopher Gibson • Marian E. Gindy • Kelly A. Hamilton • Ian Knemeyer • Kenneth A. Koeplinger • Hae Won Kwon • Traci Q. Lifsted • Karsten Menzel • Mihir Patel • Nicole Pudvah • Deanne Jackson Rudd • Jessica Seitzer • Walter R. Strapps • Thomayant Prueksaritanont • Charles D. Thompson • Jerome H. Hochman • Brian A. Carr

Received: 13 February 2014 / Accepted: 3 June 2014 / Published online: 1 July 2014

ABSTRACT

Purpose To develop a tool based on siRNA-mediated knockdown of hepatic P450 oxidoreductase (POR) to decrease the CYP-mediated metabolism of small molecule drugs that suffer from rapid metabolism *in vivo*, with the aim of improving plasma exposure of these drugs.

Methods siRNA against the POR gene was delivered using lipid nanoparticles (LNPs) into rats. The time course of POR mRNA knockdown, POR protein knockdown, and loss of POR enzyme activity was monitored. The rat livers were harvested to produce microsomes to determine the impact of POR knockdown on the metabolism of several probe substrates. Midazolam (a CYP3A substrate with high intrinsic clearance) was administered into LNP-treated rats to determine the impact of POR knockdown on midazolam pharmacokinetics.

Results Hepatic POR mRNA and protein levels were significantly reduced by administering siRNA and the maximum POR enzyme activity reduction (~85%) occurred 2 weeks post-dose. *In vitro* analysis showed significant reductions in metabolism of probe substrates due to POR knockdown in liver, and *in vivo* POR knockdown resulted in greater than 10-fold increases in midazolam plasma concentrations following oral dosing.

Conclusions Anti-POR siRNA can be used to significantly reduce hepatic metabolism by various CYPs as well as greatly increase the bioavailability of high clearance compounds following an oral dose, thus enabling it to be used as a tool to increase drug exposure *in vivo*.

KEY WORDS P450 oxidoreductase · siRNA · drug metabolism, pharmacokinetics

Electronic supplementary material The online version of this article (doi:10.1007/s11095-014-1433-0) contains supplementary material, which is available to authorized users.

R. S. Burke (✉) • I. Somasuntharam • P. Rearden • R. Eisenhandler • C. Gibson • K. A. Koeplinger • K. Menzel • N. Pudvah • D. J. Rudd • T. Prueksaritanont • C. D. Thompson • J. H. Hochman • B. A. Carr
Department of Pharmacokinetics, Pharmacodynamics, and Drug Metabolism, Merck Research Laboratories, Merck & Co., Inc., West Point, Pennsylvania 19486, USA
e-mail: rob@aviditynano.com

D. Brown • M. A. DiPietro • J. DiMuzio • K. A. Hamilton • T. Q. Lifsted • J. Seitzer • W. R. Strapps
Department of RNA Biology, Merck Research Laboratories, Merck & Co., Inc., West Point, Pennsylvania 19486, USA

S. V. Deshmukh • I. Knemeyer
Department of Pharmacokinetics, Pharmacodynamics, and Drug Metabolism, Merck Research Laboratories, Merck & Co., Inc., Boston, Massachusetts 02115, USA

S. E. Fauty • H. W. Kwon
Department of Safety Assessment and Laboratory Animal Research, Merck Research Laboratories, Merck & Co., Inc., West Point, Pennsylvania 19486, USA

M. E. Gindy • M. Patel
Department of Pharmaceutical Sciences, RNA Therapeutics, Merck Research Laboratories, Merck & Co., Inc., West Point, Pennsylvania 19486, USA

Present Address:
R. S. Burke
Department of Drug Metabolism and Pharmacokinetics, Avidity Nanomedicines, La Jolla, California 92037, USA

INTRODUCTION

During pharmaceutical drug development, early target validation and lead identification are essential for appropriate allocation of resources to drug discovery. Although *in vitro* screens can suffice for highly characterized mechanisms, generally *in vivo* pharmacodynamic (PD) studies are required to accurately assess the therapeutic potential of targets and the efficacy of lead drugs. These studies are frequently performed using unoptimized compounds with poor pharmacokinetic (PK) properties that may not generate PD effects *in vivo* simply due to insufficient exposure in target tissues. Typically, the optimization of drug properties would be achieved through medicinal chemistry, which generally requires significant time and valuable resources. Therefore, the development of tools that can increase the exposure of unoptimized compounds in target tissues is a high priority for quicker and more effective target validation and candidate drug screening.

To this end, much work has been done in an effort to block the activity of the cytochrome P450 (CYP) enzymes that are commonly responsible for metabolism of small molecule drugs in order to increase plasma and tissue exposure by decreasing clearance through metabolic pathways. Inhibition of CYP-mediated metabolism can be accomplished using the non-specific irreversible inhibitor 1-aminobenzotriazole (ABT), although this strategy is problematic since ABT has been shown to inactivate CYPs to different degrees such that some CYPs retain the majority of their activity following ABT treatment (1, 2). A more specific approach would be to use genetically modified animals where the gene for the particular CYP that mediates metabolism of the candidate drug was knocked out; however, CYP metabolic reaction phenotyping is not typically performed for preclinical species because the translation to human enzymes is not straightforward. Without knowledge of which CYP metabolizes a particular drug, it would be very difficult to knock out every CYP due to the size and diversity of the CYP multigene family. Looking upstream from the CYP enzyme activity, it is well known that cytochrome P450 oxidoreductase (POR) is one of the critical enzymes that transfers electrons to many different CYPs. These electrons enable the CYPs to metabolize small molecule drugs, so a reduction in the activity of POR could cause a reduction in the activity of multiple CYPs. Utilizing this principle, Shen *et al.* created genetically modified mice with the POR gene knocked out, but this complete deletion was shown to be embryonic lethal (3). Subsequently, two groups independently created conditional POR knockout mice using the Alb-Cre/loxP system, where the POR alleles were floxed to permit Cre-mediated excision of the POR gene and expression of the Cre recombinase was regulated by the rat albumin promoter (4, 5). Since the albumin promoter is only active in the liver postnatally, using it to drive Cre recombinase expression enables liver-specific deletion of POR following the embryonic stage where POR expression is required for survival. Mice homozygous for the deleted POR allele showed a drastically reduced capability to metabolize small molecule drugs such as pentobarbital, testosterone, and acetaminophen due to the reduced CYP activity that is a consequence of the loss of POR (4, 5). Investigations utilizing the POR knockout mice were recently extended using a panel of small molecule drugs to highlight the fact that POR deletion alters the *in vivo* pharmacokinetics of numerous drugs due to the ability of POR to transfer electrons to many different CYP enzymes (6). Although the conditional POR knockout mice were fertile and normal in terms of general appearance and behavior, these mice suffered from deleterious side effects caused by permanent POR deletion such as decreased total serum cholesterol and triglyceride levels, increased liver size and weight, increased hepatic lipid content, and reduced volume of bile acids in the gall bladder (4, 5).

The application of RNA interference is a novel approach to decrease CYP-mediated metabolism by reducing POR expression. Exogenous small interfering RNA (siRNA) can be delivered into cells where it loads into the RNA-induced silencing complex (RISC) and mediates cleavage of target mRNA transcripts. Recent work has shown that siRNA loaded into lipid nanoparticles (LNPs) will silence target genes *in vivo*, with effective gene knockdown demonstrated in the livers of rodents, non-human primates, and humans (7–11). One major advantage of using siRNA to reduce POR expression is that the effects of target gene knockdown are transient, which may help reduce some of the altered physiology noted with the permanent POR knockout mice. A second advantage of using siRNA rather than genetically modified knockout mice is that application of siRNA enables the use of more relevant preclinical species when developing drugs against disease indications unable to employ knockout mice as a disease model. In this work, LNP delivery technology was exploited to achieve potent siRNA-mediated knockdown of POR, resulting in reduced metabolism of small molecule drugs both *in vitro* and *in vivo*. Incubation of several probe substrates with rat liver microsomes *in vitro* revealed that POR knockdown reduced the metabolism mediated by several different CYPs. Oral administration of midazolam (a CYP3A substrate with high intrinsic clearance) to rats following knockdown of POR highlights that reducing midazolam metabolism generates a large increase in the

plasma exposure of midazolam. Thus, the evidence presented here comprises the foundational proof-of-concept for the use of siRNA as a tool to increase plasma exposure of small molecule drugs *in vivo*.

MATERIALS AND METHODS

Materials

All animals were obtained from Charles River Laboratories. Midazolam was purchased from Spectrum Chemical. Cells from the mouse hepatoma Hepa 1-6 cell line were obtained from the American Type Culture Collection (Cat# CRL-1830). Dulbecco's Modified Eagle Medium High Glucose with Glutamax™ (DMEM), sodium pyruvate, RNAiMax, RNA*later*, Trizol, MagMax RNA Isolation Kit, and 4–12% NuPage Bis-Tris Mini Gels were purchased from Invitrogen. The Cells-to-Ct Kit (including Lysis and Stop Reagents), TaqMan Gene Expression Master Mix, High Capacity cDNA Reverse Transcription Kit, and TaqMan Fast Advanced Master Mix were obtained from Applied Biosystems. 1-bromo-2-chloropropane was purchased from Acros Organics. Distearoylphosphatidylcholine (DSPC), cholesterol, and Cytochrome *c* Reductase (NADPH) Assay Kit were obtained from Sigma-Aldrich. Poly (ethylene glycol) 2000-dimyristoylglycerol (PEG 2000-DMG) was manufactured by NOF Corporation. SYBR gold was obtained from Molecular Probes. 1X Lysis Buffer and anti-beta-actin antibody were purchased from Cell Signaling. Anti-cytochrome P450 reductase antibody was obtained from Abcam. BCA Kit and Femto Chemi solution were obtained from Pierce. Commercial liver microsomes were prepared from male Wistar Hannover rat livers by BD Gentest. 4-hydroxydiclofenac metabolite was purchased from Fluka. Sterile saline solution for *in vivo* formulations was purchased from Teknova. All other materials were purchased from Sigma-Aldrich and used without further purification unless otherwise stated.

Design and in Vitro Screening of siRNAs

siRNA design was performed using a proprietary algorithm. In brief, the algorithm applies the following filters to candidate oligo sequences: remove oligos in the 5'-UTR; remove oligos 500 nt or more into the 3'-UTR; remove oligos with 4 or more consecutive identical bases; remove oligos containing seed-region matches to known miRNAs; remove oligos with BLAST matches to unintended transcripts; remove oligos with strong predicted seed-based off-target regulations; and remove oligos which do not match all known splice forms of the target gene. In this case, a perfect match between the mouse (NM_008898) and rat (NM_031576) transcripts of POR was also required. Remaining oligos were sorted by predicted silencing activity using a proprietary scoring method, and the top 42 were selected for screening. The two individual complementary strands of the siRNA were synthesized separately by methods previously described (12), then purified separately by ion exchange chromatography. The complementary strands were annealed and the duplex was ultrafiltered and lyophilized to form the solid drug substance. The duplex material was tested for the presence of endotoxin by standard methods.

Hepa 1–6 cells were grown in DMEM with 1 mM sodium pyruvate, 10% fetal bovine serum, 100 μg/mL streptomycin, and 100 U/mL penicillin. Cells were plated in 96-well plates at 5,000 cells/well and cultured at 37°C in the presence of 5% CO_2. In the primary screen, all 42 anti-POR siRNAs were transfected into Hepa 1–6 cells at a final siRNA concentration of 10 nM using RNAiMax according to the manufacturer's specifications. In the secondary screen, the top 12 siRNAs from the primary screen were transfected into Hepa 1–6 cells at a range of 12 concentrations with 4-fold dilutions from 40 nM to 9.5 fM. Cells were lysed 24 h after transfection and RNA was isolated by preparing lysates from the cells using Cells-to-Ct Lysis and Stop Reagents according to the manufacturer's instructions. cDNA was generated from isolated RNA in a 20 μL reaction using Reverse Transcription reagents from the Cells-to-Ct Kit according to the manufacturer's instructions. TaqMan quantitative real-time PCR analysis was performed with an ABI 7900 HT Real-Time PCR System in a 384-well plate. Reactions were set up in duplicate and one well was probed with the POR TaqMan reagents, the other with the GAPDH TaqMan reagents in a final volume of 10 μL using TaqMan Gene Expression Master Mix. All TaqMan probes and primers were purchased from Applied Biosystems as pre-validated gene expression assays. Results are calculated by the comparative Ct method, where the difference between the POR Ct value and the GAPDH Ct value (ΔCt) is calculated and then further normalized relative to the PBS control by taking a second difference (ΔΔCt), as described previously (13).

Formulation of siRNAs into LNPs

LNPs were prepared *via* the rapid precipitation process as previously described (14), with modifications as follows. LNPs were assembled by micro-mixing appropriate volumes of an organic solution of lipids with an aqueous solution containing siRNA duplexes. The lipid solution was prepared by dissolving Merck's proprietary cationic lipid, cholesterol, DSPC and PEG 2000-DMG, with a molar ratio of 58:30:10:2, in ethanol. siRNA duplexes were prepared in an aqueous citrate buffer (pH 5) using an siRNA to cationic lipid molar ratio of 0.17. Reagent solutions were delivered at nearly equal volumetric flow rates to the inlet of a confined volume

T-mixer device using syringe pumps (Harvard Apparatus PHD 2000). The mixed material was sequentially diluted into equal volumes of citrate buffer (pH 6) and PBS in a multi-stage in-line mixing process. Following buffer dilutions, LNPs were purified to remove free siRNA *via* anion exchange chromatography. The residual ethanol was removed and the buffer was exchanged into a buffer suitable for cryo-preservation *via* tangential flow diafiltration. Finally, LNPs were concentrated to the target siRNA concentration, sterilized by filtration *via* 0.2 μm sterile filter, vialed under aseptic conditions, and frozen for storage at -20°C. LNP size and size distribution were determined following freeze/thaw by dynamic light scattering using a DynaPro particle sizer (Wyatt Technology). For these LNP formulations, the average particle diameter was 80 ± 1 nm with a particle distribution index of 0.15 ± 0.03. The efficiency of siRNA encapsulation in LNPs was determined by the SYBR gold fluorimetric method and was greater than 90% for all preparations.

In Vivo Screening of siRNAs

All animal studies were conducted following protocols in accordance with the Institutional Animal Care and Use Committee (IACUC) at Merck, which adhere to the regulations outlined in the USDA Animal Welfare Act as well as the "Principles of Laboratory Animal Care" (NIH publication #85-23, revised in 1985). LNPs containing anti-POR siRNAs were dosed into groups ($n=3$) of female CD-1 mice and male Wistar Hannover rats at 0.01, 0.03, 0.1, and 0.3 mg/kg (based on weight of siRNA) by i.v. injection into the tail vein. The i.v. injection was done as a bolus of approximately 5 mL/kg for mice and 1 mL/kg for rats. Control LNP containing scrambled siRNA (a nonsense sequence designed to have no activity) was dosed at 0.3 mg/kg into one group ($n=3$) of animals and a sham dose of PBS vehicle was injected at matched dose volumes in another group ($n=3$). 2 days post-dose, the animals were sacrificed by CO_2 asphyxiation and 3 mm liver punches were collected, preserved in RNA*later*, and stored at 4°C. The liver samples were homogenized in Trizol using a bead mill tissue lyser (Qiagen); disruption was performed for two 5-min cycles at 30 Hz. RNA extraction was performed using 1-bromo-2-chloropropane and total RNA was isolated from the aqueous phase using the MagMax RNA Isolation Kit. RNA (125 ng) was reverse transcribed using the High Capacity cDNA Reverse Transcription Kit. TaqMan qPCR analysis was performed with an ABI 7900 Real-Time PCR System using TaqMan Fast Advanced Master Mix. All TaqMan probes and primers for POR and PPIB (housekeeping gene) were purchased from Applied Biosystems as pre-validated gene expression assays. Results are calculated by the comparative Ct method, where the difference between the POR Ct value and the PPIB Ct value (ΔCt) is calculated and then further normalized relative to the PBS control by taking a second difference (ΔΔCt), as described previously (13).

Time Course of POR Knockdown

LNPs containing anti-POR siRNA-04 were dosed into groups ($n=3$) of male Wistar Hannover rats at 0.5 mg/kg (based on the weight of siRNA) by i.v. injection of a bolus of approximately 1 mL/kg into the tail vein. Control LNP containing scrambled siRNA was dosed at 0.5 mg/kg into one group ($n=3$) of rats and a sham dose of PBS vehicle was injected at matched dose volumes in another group ($n=3$). At various harvest times post-dose, the animals were sacrificed by CO_2 asphyxiation and the livers were perfused *in situ* with cold PBS to remove any blood. Liver tissue punches were collected and analyzed by qPCR as described above to determine extent of POR mRNA knockdown. In addition, 50 mg punches from the rat livers were used in western blots to determine POR protein levels as described below. Finally, the remaining liver tissue was used to generate liver microsomes to probe POR enzyme activity as described below.

Western Blot for POR Protein

Tissue samples were homogenized in 0.5 mL of 1X Lysis Buffer with protease inhibitor cocktail in 96-deep well plates containing one bead per well for 5 min using a Geno/Grinder® 2000 (SPEX Sample Prep) at 1,200 rpm at 4°C. The homogenates were centrifuged at 12,000 rpm at 4°C for 20 min to obtain the supernatant and protein concentrations were determined using a BCA Kit. Protein samples (40 μg) were loaded on 4–12% NuPage Bis-Tris Mini Gels, separated by SDS-PAGE under reducing conditions, and transferred to PVDF membranes using an XCell II™ Blot Module (Invitrogen). Membranes were blocked with 5% BSA in TBST (Tris-buffered saline and 0.1% Tween-20) followed by incubation with either anti-cytochrome P450 reductase or anti-beta-actin primary antibodies at 1:1,000 dilution overnight at 4°C. Membranes were washed three times in TBST and incubated with appropriate secondary antibodies conjugated to horseradish peroxidase at 1:4,000 dilution for 1 h at room temperature. Membranes were once again washed three times with TBST, incubated for 5 min in Femto Chemi solution, and then visualized using a FluorChem Q MultiImage III (Alpha Innotech).

POR Enzyme Activity

One piece of liver (~3 g) from each animal in a treatment group ($n=3$) were pooled together (total liver tissue weight ~9 g) and frozen at -80°C until use. Pooled liver samples were homogenized in four volumes of 0.15 M KCl buffered with 50 mM Tris–HCl, pH 7.4 (containing protease inhibitor

cocktail) using a glass/Teflon Potter-Elvehjem tissue homogenizer and centrifuged for 20 min at 6,000*g* at 4°C. Pellets were discarded and the supernatant was centrifuged for an additional 20 min at 18,000*g* to ensure removal of mitochondria. The supernatant (S9 fraction) was collected and centrifuged for 75 min at 105,000*g* in a Beckman Optima LI-80 K ultracentrifuge at 4°C. The resulting microsomal pellet was washed and re-centrifuged for 30 min at 105,000*g* to collect microsomes in a minimal volume of 0.25 M sucrose buffered by 50 mM Tris–HCl, pH 7.4. Protein concentrations were determined using a BCA Kit and microsomes were stored at a concentration of 10 mg/mL at -80°C until use.

POR enzyme activity was measured using the Cytochrome *c* Reductase (NADPH) Assay Kit. Cytochrome *c* reduction was measured for rat liver microsomes derived from each terminal harvest time point as well as PBS treated rats and commercial male Wistar Hannover rat liver microsomes as controls. All measurements were made using a concentration of 0.1 mg/mL microsomal protein and 100 μM NADPH in buffer (0.3 M phosphate with 0.1 mM EDTA at pH 7.8) at 25°C. The reduction of cytochrome *c* by POR was measured by following the increase in absorbance at 550 nm on a DU 800 spectrophotometer (Beckman Coulter) for 5 min immediately following the addition of NADPH to the reaction. The activity of POR was calculated according to the manufacturer's instructions and then normalized to the activity determined for the PBS control group.

LC-MS/MS Assay

Samples were protein crashed by transfer into 96-well plates containing 3 volumes of acetonitrile with 0.1% (v/v) formic acid and an internal standard (200 nM of labetalol, 200 nM of alprazolam, or 200 nM of imipramine). The crash plates were vortex mixed and centrifuged at 4°C for 20 min at 3,800 rpm. A 100 μL aliquot of the resulting supernatant was diluted with an equal volume of 0.1% (v/v) formic acid in water to prepare samples for injection onto the LC-MS/MS system. Samples were first separated on a C_{18} column using a gradient of water containing 0.1% formic acid (solvent A) and acetonitrile containing 0.1% formic acid (solvent B), followed by analysis on a Sciex API-4000 or API-5000 QQQ mass spectrometer utilizing an ESI source and operated in either negative or positive ion mode. Quantitation in negative ion mode was performed by monitoring transitions m/z 294.0 to 250.0 for diclofenac, m/z 311.7 to 268.0 for 4-hydroxydiclofenac, and m/z 327.0 to 309.0 for labetalol. Quantitation in positive ion mode was performed by monitoring transitions m/z 326.2 to 291.1 for midazolam, m/z 296.2 to 213.9 for diclofenac, m/z 262.3 to 188.1 for bufuralol, m/z 455.2 to 165.0 for verapamil, m/z 309.1 to 205.1 for alprazolam, m/z 281.3 to 193.1 for imipramine, and m/z 329.1 to 162.1 for labetalol. Data reduction, including peak integration, was performed with MultiQuant software (version 2.1.1; AB Sciex).

Enzyme Kinetics of Diclofenac Metabolism

Diclofenac was incubated with microsomes to enable formation of a 4-hydroxydiclofenac metabolite by CYP-mediated hydroxylation reactions. Commercial male Wistar Hannover rat liver microsomes and microsomes from livers harvested 14 days post-dose of LNP-04 (0.5 mg/kg of anti-POR siRNA-04) were used in the incubations at 0.25 mg/mL of microsomal protein. Diclofenac was added to the incubations at final concentrations ranging from 0.01 to 50 μM in a buffer containing 100 mM PO_4 and 50 mM $MgCl_2$ at pH 7.4. The reactions were initiated by adding NADPH at a final concentration of 1 mM and carried out in a shaker incubator at 37°C for 10 min. The incubations also included samples where NADPH was not added to the reaction mix in order to control for any non-NADPH-mediated product formation. Samples were processed and analyzed by LC-MS/MS as described above. The peak-area-ratio of metabolite to internal standard was calculated and compared to a standard curve generated by spiking the 4-hydroxydiclofenac metabolite into the same rat liver microsomes used in the incubation. The amount of metabolite formed was divided by the time of the incubation and the amount of microsomal protein to generate the velocity units of pmol/min/mg protein. The data were then fit to the Michaelis-Menten equation:

$$v = \frac{V_{max} \cdot [S]}{K_m + [S]} \quad (1)$$

where v is the velocity of the hydroxylation reaction, V_{max} is the maximum reaction velocity, [S] is the substrate (diclofenac) concentration, and K_m is a constant equal to the substrate concentration that generates a reaction velocity that is half of V_{max}. Under saturating conditions, the following relationship is also true:

$$V_{max} = k_{cat} \cdot [E]_0 \quad (2)$$

where $[E]_0$ is the total enzyme concentration and k_{cat} is the rate constant of the hydroxylation reaction once the substrate is bound to the CYP enzyme. The parameters K_m and V_{max} were determined by nonlinear regression analysis using GraphPad Prism software (version 5.0).

Preparation of Liver and Intestinal Microsomes

In order to determine the relative contributions of the liver and gut to overall metabolism, liver and intestinal microsomes were prepared from the same rats. LNPs containing anti-POR siRNA-04 were dosed into one group ($n=3$) of male Wistar Hannover rats at 1 mg/kg (based on the weight of siRNA) by i.v. injection of a bolus of approximately 1 mL/kg into the tail vein. Control LNP containing scrambled siRNA was dosed at 1 mg/kg into one group ($n=3$) of rats and a sham dose of PBS

vehicle was injected at matched dose volumes in another group ($n=3$). Dosing was performed at Merck and animals were housed on-site for 2 weeks. On the 14th day post-dose, treated rats were shipped to BioreclamationIVT (Baltimore, MD). The rat livers and intestines (harvested from the same animals) were used to make microsomes according to BioreclamationIVT's standard protocol (similar to the microsome protocol described above).

Midazolam Maleate Salt Formation

Given the poor aqueous solubility of the neutral form of midazolam, the midazolam maleate salt was produced based on the protocol of Walser and coworkers to enable dissolution of midazolam directly in saline solution (15, 16). Midazolam (1.0 mmol) and ethanol (0.552 mL) were added to a round-bottom flask and the suspension was heated to 50°C. Once the midazolam was dissolved, a solution of maleic acid (1.09 mmol) in ethanol (0.463 mL), which had been warmed to 50°C, was slowly added. The reaction mixture was stirred for an additional 5 min and then allowed to cool to room temperature. After 4 h, diethyl ether (2.30 mL) was added dropwise to the reaction flask and the white solid was filtered off. The solid was dried under vacuum for 16 h at room temperature and an additional 4 h at 90°C. A total of 0.9 mmol midazolam maleate was isolated and used in all subsequent studies.

In Vitro Microsomal Stability

Midazolam and diclofenac (each at 0.2 μM) were separately incubated with male Wistar Hannover rat liver microsomes (from treated animals) using 0.1 and 0.25 mg/mL of microsomal protein, respectively, in 100 mM PO_4 buffer with 50 mM $MgCl_2$ at pH 7.4. The reaction was initiated with the addition of NADPH to a final concentration of 1 mM and carried out in a shaking water bath at 37°C. Aliquots were removed at t=0 and six subsequent time points (2, 5, 7, 10, 12, and 15 min for midazolam and 5, 10, 15, 20, 30, and 40 min for diclofenac) for processing and analysis by LC-MS/MS as described above. The analyte to internal standard peak-area-ratios (PAR) were converted to percentage of parent drug remaining (%R) using the t=0 PAR value as 100%. The elimination rate constant ($-k_e$) in liver microsomes was determined as the slope of the linear regression from ln (%R) *versus* incubation time relationships. Similar to Obach and coworkers (17, 18), the rate constant k_e (with units of min^{-1}) was then used to calculate apparent intrinsic clearance ($CL_{int,app}$) using the following equation:

$$CL_{int,app} = k_e \times \frac{mL\ incubation}{mg\ microsomal\ protein} \times \frac{45\ mg\ microsomal\ protein}{g\ liver\ weight} \times \frac{40\ g\ liver\ weight}{kg\ body\ weight} \quad (3)$$

where the mg microsomal protein per g liver weight and the g liver weight per kg body weight are constants that have been determined empirically for rats.

Midazolam and diclofenac (each at 0.2 μM) were separately incubated with male Wistar Hannover rat intestinal microsomes (from treated animals) using 2 mg/mL of microsomal protein in 100 mM PO_4 buffer with 50 mM $MgCl_2$ at pH 7.4. The reaction was initiated with the addition of NADPH to a final concentration of 1 mM and carried out in a shaking water bath at 37°C. Aliquots were removed at t=0 and six subsequent time points (5, 10, 20, 30, 40, and 60 min) for processing and analysis by LC-MS/MS as described above. The analyte to internal standard peak-area-ratios (PAR) were converted to percentage of parent drug remaining (%R) using the t=0 PAR value as 100%.

Plasma Protein Binding, Microsomal Protein Binding, and Blood-to-Plasma Ratio

Binding of midazolam to proteins in fresh Wistar Hannover rat plasma was determined using an equilibrium dialysis method. Fresh rat blood was collected over EDTA from 3 donors, pooled, and centrifuged for 12 min at 3,000 rpm, 4°C to collect plasma. Incubation buffer (100 mM sodium phosphate with 150 mM sodium chloride, pH 7.4) was added to one side of a Thermo Scientific Rapid Equilibrium Dialysis Device (with 8 kDa MWCO membrane) and fresh rat plasma containing 2 μM of midazolam was added to the other side. Samples were incubated for 6 h at 37°C, 5% CO_2 on a plate shaker and then removed from the device for processing and analysis by LC-MS/MS as described above. At the protein crash step, all samples were matrix-matched by adding an equal volume of the opposite matrix. The concentration of midazolam in both the buffer and plasma samples was determined by calculating the peak-area-ratio of midazolam to internal standard and comparing to a standard curve prepared in the same rat plasma used in the incubation. The extent of plasma protein binding is expressed as the fraction unbound in plasma ($f_{u,p}$) and is calculated as the ratio of the midazolam concentration in the buffer to the midazolam concentration in the plasma. A value of $f_{u,p}=0.04\pm0.002$ was determined for midazolam.

Binding of midazolam to proteins in commercial male Wistar Hannover rat liver microsomes was determined by an equilibrium dialysis method similar to that used for plasma

protein binding. Incubation buffer (100 mM PO_4 with 50 mM $MgCl_2$, pH 7.4) was added to one side of the device and rat liver microsomes matrix (0.5 mg/mL of microsomal protein in the same incubation buffer) containing 2 μM of midazolam was added to the other side. The samples were dialyzed, processed, and analyzed by LC-MS/MS as described above. The concentration of midazolam in both the buffer and microsome samples was determined by calculating the peak-area-ratio of midazolam to internal standard and comparing to a standard curve prepared in the same rat liver microsomes used in the incubation. The extent of microsomal protein binding is expressed as the fraction unbound in microsomes ($f_{u,mic}$) and is calculated as the ratio of the midazolam concentration in buffer to the midazolam concentration in microsomes. A value of $f_{u,mic} = 0.89 \pm 0.03$ was determined for midazolam.

In order to determine the blood to plasma ratio of midazolam, fresh Wistar Hannover rat blood was collected over EDTA from 3 donors and pooled. Midazolam was added to pooled whole blood at a final concentration of 2 μM and incubated for 30 min at 37°C in a shaking water bath. Following incubation, the blood was centrifuged to generate plasma. Aliquots of the resulting plasma were processed and analyzed by LC-MS/MS as described above, and they serve as the "plasma" samples in the blood to plasma ratio. A separate fraction of the pooled whole blood was centrifuged to generate plasma. Midazolam was added to an aliquot of this plasma at a final concentration of 2 μM and incubated for 30 min at 37°C in a shaking water bath. Following incubation, aliquots of the plasma were processed and analyzed by LC-MS/MS as described above, and they serve as the "blood" samples in the blood to plasma ratio. The concentration of midazolam in the samples was determined by calculating the peak-area-ratio of midazolam to internal standard and comparing to a standard curve prepared in the same rat plasma used in the incubation. The blood to plasma ratio (B/P) was calculated by dividing the concentration of midazolam in each of four "blood" samples by the concentration in each of four "plasma" samples (16 total measurements). A value of (B/P) = 0.81 ± 0.02 was determined for midazolam.

In Vivo Midazolam PK

An initial dose response study was performed using pre-cannulated (jugular vein cannula) male Wistar Hannover rats. Midazolam was dissolved in sterile saline solution at appropriate concentrations to achieve dose volumes of 2 mL/kg. Midazolam was dosed i.v. at 0.03, 0.1, 0.3, 1, and 3 mg/kg and dosed p.o. at 1, 3, and 10 mg/kg (with n = 4 rats per group). At specific time points up to 24 h post-dose, 250 μL of blood was collected from the cannula and centrifuged to generate plasma. Aliquots of the plasma samples (50 μL) were processed and analyzed by LC-MS/MS as described above. Midazolam concentrations in plasma were determined by calculating the peak-area-ratio of midazolam to internal standard and comparing to a standard curve prepared in untreated Wistar Hannover rat plasma. Pharmacokinetic analysis was performed in Watson Bioanalytical LIMS (version 7.3; Thermo Fisher Scientific) with a model-independent calculation method.

A second study was conducted to determine the effect of POR knockdown on midazolam PK. Male Wistar Hannover rats were separated into three treatment groups ($n = 8$ each) and received an i.v. dose *via* the tail vein of LNP-04 containing anti-POR siRNA-04, control LNP containing scrambled siRNA, or a sham dose of PBS vehicle. Both LNPs were dosed at 1 mg/kg (based on the weight of siRNA) *via* a bolus of approximately 1 mL/kg and the dosing volume of PBS was matched. 13 days after the LNP and PBS doses, the rats were anesthetized and surgically cannulated in the jugular vein, with the end of the catheter remaining externalized for drug administration and blood sampling. The following day (14 days after LNP dose, when reduction in POR enzyme activity is maximal) the rats in each treatment group were subdivided into two subgroups ($n = 4$ each) where one subgroup received an i.v. dose of midazolam at 0.5 mg/kg and the other subgroup received a p.o. dose of midazolam at 10 mg/kg. Following administration of midazolam, 250 μL of blood was collected and centrifuged to generate plasma at specified time points out to 24 h. After the completion of the blood sampling (a total of 15 days post-dose of LNP or PBS), animals were sacrificed by CO_2. Livers were harvested and samples were collected as described above. Small intestines were excised, perfused with 25 mL of saline solution, and then separated into segments of the duodenum and jejunum. The duodenum and jejunum were separately scraped to remove the mucosal layer from the smooth muscle layer; the mucosal layers (that contain enterocytes, which are the cells in the gut that highly express drug metabolizing enzymes) were collected in vials, snap frozen, and stored at -80°C until use. Both liver and small intestine samples were homogenized and processed for mRNA knockdown determination as described above. Midazolam concentrations in plasma were determined and pharmacokinetic analysis was performed as described above.

RESULTS

Selection of Anti-POR siRNA Sequences

Forty-two different siRNAs against the POR gene were transfected into mouse Hepa 1-6 cells *in vitro* at a single concentration (10 nM) and screened for maximum mRNA knockdown of the POR transcript (data not shown). The top 12 sequences were further analyzed in dose–response format

in vitro, and the four siRNAs with the lowest IC_{50} and highest POR mRNA knockdown were then formulated into lipid nanoparticles (LNPs) for screening *in vivo*. These four LNPs containing the best anti-POR siRNAs (Table I) were dosed into mice and rats at doses ranging from 0.01 mg/kg to 0.3 mg/kg (dose based on the weight of siRNA) and mRNA knockdown in the liver was determined 48 h post-dose as shown in Fig. 1. The *in vivo* dose response curves show LNP-04 (containing anti-POR siRNA-04) performed the best in both species (in terms of ED_{50} as well as maximum knockdown) and there was slightly better activity in rats (Fig. 1B) compared to mice (Fig. 1A). In rats, LNP-04 achieved 93% knockdown of POR mRNA in liver at the highest tested dose of 0.3 mg/kg. In both species, a negative control LNP (with scrambled siRNA that has a nonsense sequence designed to have no activity) was dosed at 0.3 mg/kg and showed no mRNA knockdown, illustrating that the change in POR mRNA expression was due to specific silencing generated by the anti-POR siRNAs. Since LNP-04 provided the highest POR mRNA knockdown in both species, it was used for the remainder of the studies presented in this work.

Effects of Anti-POR siRNA Treatment

The time course of POR mRNA knockdown, protein knockdown, and loss of POR enzyme activity was determined in male Wistar Hannover rats (a preferred preclinical species for *in vivo* drug metabolism studies) following injection of LNPs (0.5 mg/kg of siRNA) or a sham dose of PBS as shown in Fig. 2. Administration of LNP-04 led to very rapid POR mRNA knockdown in liver (Fig. 2A) with greater than 90% knockdown as early as 24 h post-dose. The knockdown is maintained at 90% out to 7 days (168 h) post-dose and then the mRNA knockdown begins to show a rebounding trend by 14 days post-dose (336 h). In contrast, the POR protein takes much longer to reach maximum knockdown in liver, finally achieving 79% and 84% protein reduction at 1 week and 2 weeks post-dose, respectively (Figs. 2b and c). The livers from the rats in each group ($n=3$) were pooled and processed into microsomes. Since POR is known to reduce cytochrome c, these liver microsomes were tested in a cytochrome c reduction assay to determine POR enzyme activity (Fig. 2D). The loss in POR enzyme activity roughly parallels the loss of POR protein from the tissue and by 2 weeks post-dose the POR activity was reduced by 84%, which is perfectly consistent with the reduction in protein levels. In the following studies, the effects of POR knockdown were assessed 2 weeks post-dose of LNPs to provide enough time for maximum loss of POR protein and enzyme activity from the liver.

In Vitro Metabolism

The impact of POR knockdown on CYP activity was evaluated by incubating liver microsomes with diclofenac and monitoring the formation of the metabolite 4-hydroxydiclofenac over time (Fig. 3). Both commercial microsomes (prepared from livers of untreated rats) and treated microsomes (prepared from rat livers 14 days post-dose of LNP-04 with 0.5 mg/kg of anti-POR siRNA-04) were used. Fitting the data in Fig. 3 to the equation describing Michealis-Menten kinetics (eq. 1), it was determined that for commercial microsomes the formation of 4-hydroxydiclofenac had a K_m

Table I The Top 4 Candidate Anti-POR siRNAs and the Scrambled Control siRNA that were Formulated into LNPs for *In Vivo* Screening.Letters Within the Circle Represent the Base in the Sequence. The Color of the Circle Represents the Chemical Modification on the 2'-ribose Sugar Position: Red = ribose (2'-OH); Blue = deoxy (2'-H); Green = fluoro (2'-F); Black = O-methyl (2'-OCH_3). The Red Triangles Represent Inverted Abasic Residues.

siRNA Description	Passenger Strand (top, 5' to 3') Guide Strand (bottom, 3' to 5')
anti-POR siRNA-01	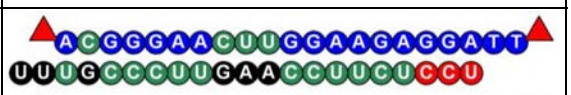
anti-POR siRNA-02	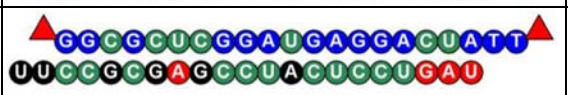
anti-POR siRNA-03	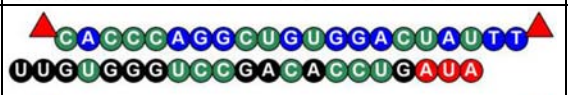
anti-POR siRNA-04	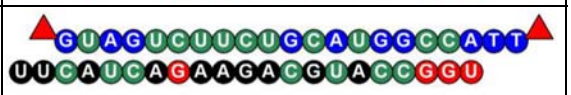
scrambled siRNA	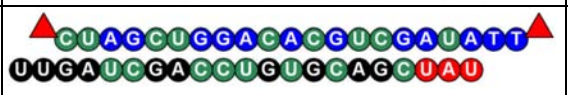

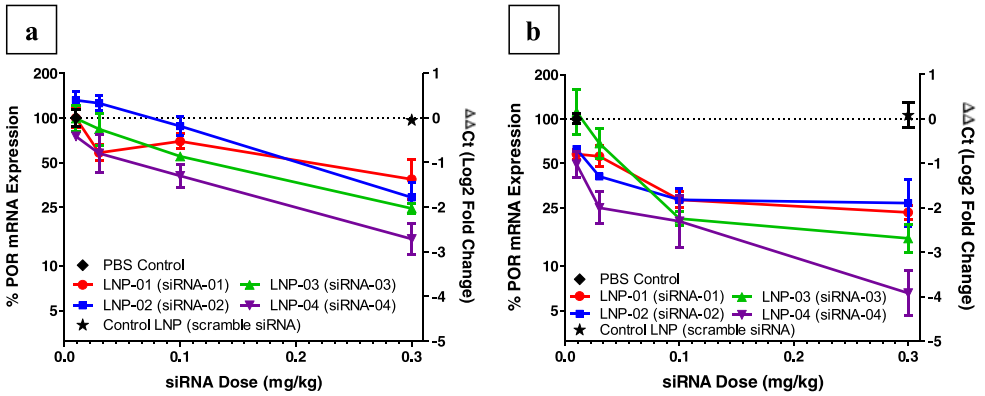

Fig. 1 POR mRNA knockdown in the livers of (**A**) female CD-1 mice and (**B**) male Wistar Hannover rats 48 h post-dose following i.v. administration of PBS or LNPs containing the lead anti-POR siRNAs or scrambled siRNA at dose levels from 0.01 to 0.3 mg/kg. POR mRNA levels are normalized to mRNA levels of the housekeeping gene Ppib and all data are normalized relative to 100% expression for PBS control group. Groups were $n=3$ animals and data are expressed as mean ± S.E.M.

of 13.5±3.0 μM and a V_{max} of 1707±155 pmol/min/mg protein. While the treated microsomes had a similar K_m of 11.7±2.5 μM for the formation of 4-hydroxydiclofenac, the V_{max} was found to be only 527±44 pmol/min/mg protein. Using the extra sum-of-squares F test to compare the two sets of microsomes, it was determined that the K_m values were statistically the same ($p=0.783$) and the V_{max} values were statistically significantly different ($p<0.001$). The more than

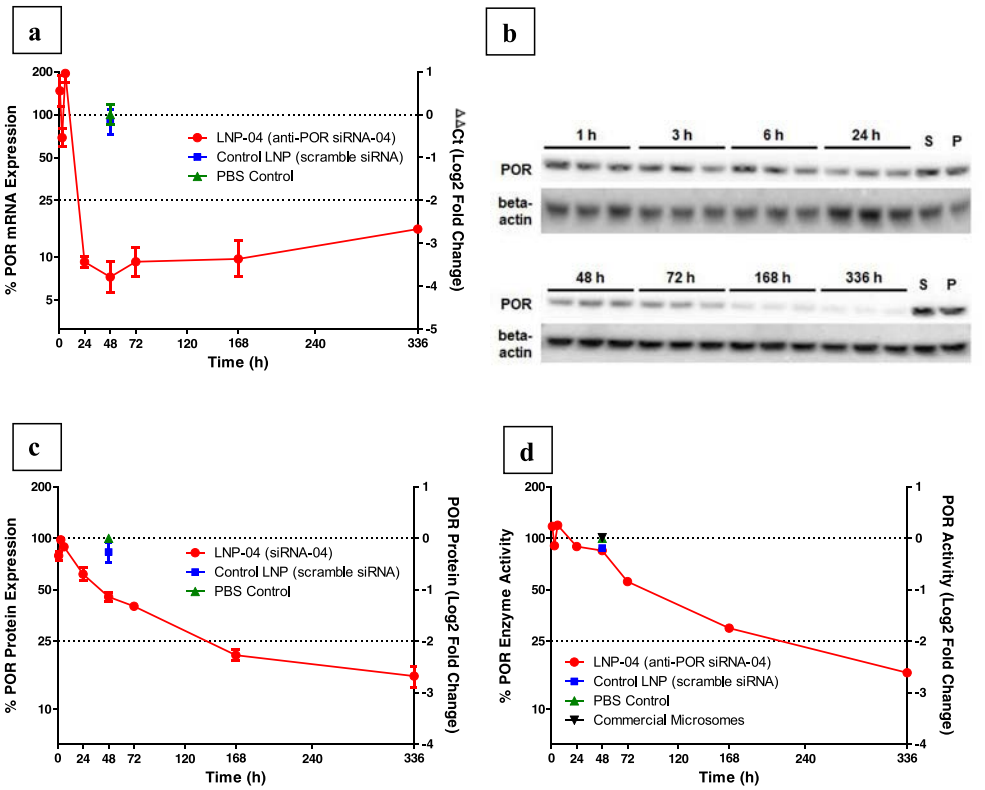

Fig. 2 The effects on POR following an i.v. dose of PBS or LNPs (0.5 mg/kg siRNA; either anti-POR siRNA-04 or scrambled siRNA) into male Wistar Hannover rats. (**A**) Time course of POR mRNA knockdown in liver. POR mRNA levels are normalized to mRNA levels of the housekeeping gene Ppib and all data are normalized relative to 100% expression for PBS control group. Groups were $n=3$ rats and data are expressed as mean ± S.E.M. (**B**) Western blot showing the loss of POR protein from liver over time, with detection of the POR protein at 78 kDa and detection of β-actin at 45 kDa. Controls in the right two lanes are abbreviated "S" for scrambled siRNA and "P" for PBS control. (**C**) Time course of POR protein knockdown in liver as determined by quantification of the POR gel bands normalized to the β-actin gel bands. Groups were $n=3$ and data are expressed as mean ± S.E.M. (**D**) Time course of POR enzyme activity in liver, determined as the amount of cytochrome c reduction mediated by microsomes produced from livers of treated animals (or commercial microsomes from untreated rats). Livers from each group were pooled into a single microsomal preparation and activity was normalized to the activity determined for the PBS control group.

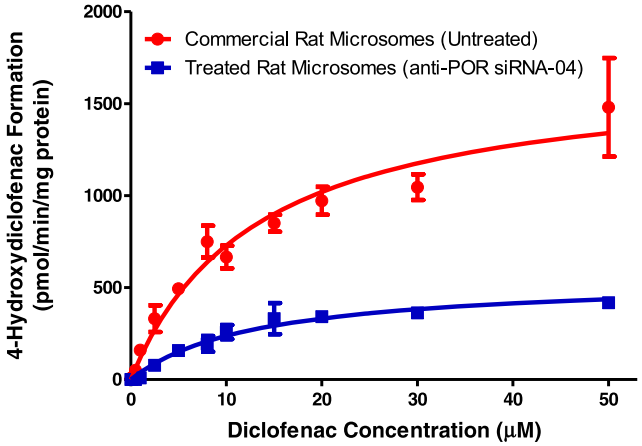

Fig. 3 Metabolism of diclofenac into 4-hydroxydiclofenac during 10 min incubations at 37°C with rat liver microsomes using concentrations of diclofenac from 0.01 to 50 μM and 0.25 mg/mL of microsomal protein. Commercial rat microsomes were prepared from livers of untreated rats, and treated rat microsomes were prepared from livers of rats 14 days post-dose of LNP-04. Data are expressed as mean ± S.E.M. of 2 replicates. Data were fit to Michaelis-Menten kinetics (eq. 1) using nonlinear regression and the best fit curves are shown for both data sets.

3-fold decrease in V_{max} following POR knockdown illustrates that loss of POR activity results in reduced CYP-mediated diclofenac metabolism.

In order to determine the relative impact of POR knockdown on drug metabolism in liver and gut, male Wistar Hannover rats were dosed with LNPs (1 mg/kg of siRNA; either LNP-04 containing anti-POR siRNA-04 or control LNP containing scrambled siRNA) or PBS, and both liver and small intestine were harvested two weeks post-dose from the same rats for the production of microsomes. Incubation of diclofenac and midazolam with the liver microsomes prepared from animals treated with control LNP or PBS resulted in considerable metabolism of both substrates, but the metabolism was significantly decreased during incubation with the liver microsomes prepared from animals treated with LNP-04 containing anti-POR siRNA-04 (Fig. 4). The curves in Fig. 4 were fit by linear regression and the slopes were compared using the extra sum-of-squares F test. For both midazolam and diclofenac, it was determined that POR knockdown statistically significantly altered the slope of the ln (%R) *versus* time curve ($p<0.0001$), regardless of which control group was used as a comparator. Since the concentration of NADPH was in great excess to the concentration of both substrates during the microsomal incubations, the NADPH concentration was assumed constant and the pseudo-first-order rate constant k_e was determined from the negative slope of the ln (%R) *versus* time plot. The apparent intrinsic clearance of diclofenac in each rat liver microsome preparation was then calculated using k_e and eq. 3, with $CL_{int,app}$ determined to be 1428 ± 259 mL/min/kg for liver microsomes from rats treated with PBS, 1892 ± 20 mL/min/kg for liver microsomes from rats treated with control LNP, and 276 ± 9 mL/min/kg for liver microsomes from rats treated with LNP-04 containing anti-POR siRNA-04. The apparent intrinsic clearance of midazolam was calculated similarly, with $CL_{int,app}$ determined to be 3551 ± 380 mL/min/kg for liver microsomes from rats treated with PBS, 3593 ± 260 mL/min/kg for liver microsomes from rats treated with control LNP, and 406 ± 23 mL/min/kg for liver microsomes from rats treated with LNP-04 containing anti-POR siRNA-04. Both substrates have a high apparent intrinsic clearance in normal rat liver microsomes, with the $CL_{int,app}$ of midazolam approximately 2-fold higher than the $CL_{int,app}$ of diclofenac. The knockdown of POR results in a decrease in the apparent intrinsic clearance (compared to PBS microsomes) of approximately 5-fold for diclofenac and approximately 9-fold for midazolam. Other substrates (verapamil and bufuralol) were also incubated in these liver microsome preparations with similar results (data not shown), highlighting that POR knockdown reduces the liver metabolism of many small molecule drugs. In contrast, the intestinal microsome preparations showed no metabolism of diclofenac or midazolam, even when used at microsomal protein concentrations much higher than those used in the liver microsome incubations (data not shown). Midazolam was used in the following *in vivo* studies because it had the highest intrinsic clearance and showed the largest reduction in clearance following POR knockdown.

Midazolam PK in Untreated Rats

PK linearity of midazolam was evaluated by administering midazolam at various dose levels into untreated male Wistar Hannover rats (obtained pre-cannulated in jugular vein) *via* both intravenous (i.v.) and oral (p.o.) routes. Mean plasma concentration-time curves of midazolam are shown in Fig. 5 and associated PK parameters are presented in Table II. The dose-normalized AUC was calculated for each dose level and averaged within each dose route, with the bioavailability (F) calculated as the ratio of dose-normalized AUC for the p.o. route to dose-normalized AUC for the i.v. route. The determined value of F = 0.02 reveals that midazolam has very poor oral bioavailability in rats, highlighted by the fact that the plasma concentrations for the 1 mg/kg p.o. dose were very close to the lower limit of quantitation for the LC-MS/MS assay. Following i.v. dosing, midazolam appears to have a roughly dose-proportional increase in AUC for doses between 0.03 to 1 mg/kg. Based on these findings, a 10 mg/kg oral dose was chosen for the subsequent studies and a 0.5 mg/kg dose for the i.v. route was chosen to roughly match the plasma AUCs.

Midazolam PK in Treated Rats

Male Wistar Hannover rats were pretreated with intravenous injections of LNPs (1 mg/kg of siRNA) or a sham PBS dose.

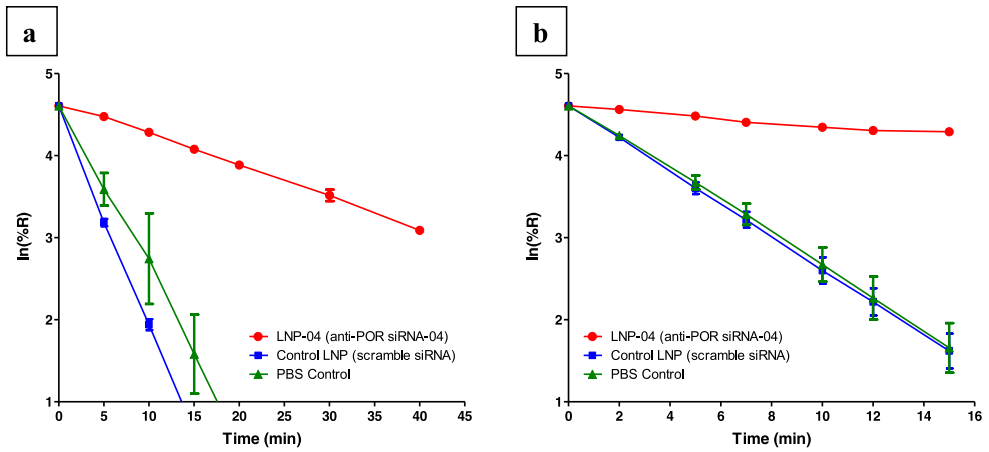

Fig. 4 Metabolism of (**A**) diclofenac and (**B**) midazolam during incubation with male Wistar Hannover rat liver microsomes prepared 14 days after treatment with LNPs or PBS. Diclofenac was incubated at 0.2 μM with 0.25 mg/mL of microsomal protein at 37°C for up to 40 min. Midazolam was incubated at 0.2 μM with 0.1 mg/mL of microsomal protein at 37°C for up to 15 min. The percentage of parent drug remaining (%R) was calculated using the t = 0 value as 100%. Data are expressed as mean ± S.E.M. of 3 replicates.

After waiting 14 days following the pretreatment, the rats either received an i.v. dose of midazolam at 0.5 mg/kg or a p.o. dose of midazolam at 10 mg/kg. Mean plasma concentration-time curves of midazolam are shown in Fig. 6 and associated PK parameters are presented in Table III. Interestingly, knockdown of POR appears to have a relatively small impact on the plasma PK of midazolam following an i.v. dose, as the administration of LNP-04 only leads to a 1.4-fold increase in midazolam plasma AUC compared to PBS treatment ($p < 0.05$ when comparing the AUCs using Student's *t*-test). Following p.o. administration of midazolam, in contrast, the plasma PK in rats with POR knockdown shows a 20-fold increase in midazolam plasma AUC compared to the animals treated with PBS ($p < 0.02$ when comparing the AUCs using Student's *t*-test). The bioavailability (F) of the oral dose of midazolam was determined to be 0.02 for rats pretreated with PBS (matches the value calculated above in the dose–response experiment) and 0.28 for rats pretreated with LNP-04. Thus, the knockdown of POR produced a 14-fold increase in the bioavailability of midazolam following a 10 mg/kg p.o. dose, which is a major driver of the 20-fold increase in plasma AUC. With less than 2-fold changes to PK parameters following i.v. administration of midazolam and greater than 10-fold changes to PK parameters following p.o. administration of midazolam, it is evident that POR knockdown generates very different responses depending on the route of administration for midazolam.

Following the completion of the PK sampling (a total of 15 days post-dose of LNP or PBS), mRNA knockdown was measured in the liver and in the mucosal layers of the small intestine, as shown in Fig. 7. Consistent with previous data, the 1 mg/kg dose of anti-POR siRNA-04 (in LNP-04) produced approximately 90% POR mRNA knockdown in the liver while the control LNP and PBS had no effect on POR mRNA ($p < 0.0001$ when comparing the anti-POR LNP to control LNP using Student's *t*-test). Conversely, there was no POR knockdown in the mucosal layer of either the duodenum or the jejunum, highlighting the liver specificity of the LNP delivery system ($p > 0.5$ when comparing the anti-POR LNP to control LNP in both jejunum and duodenum using Student's *t*-test). Due to the fact that there is no change in the expression of POR in the gut, the measured differences in

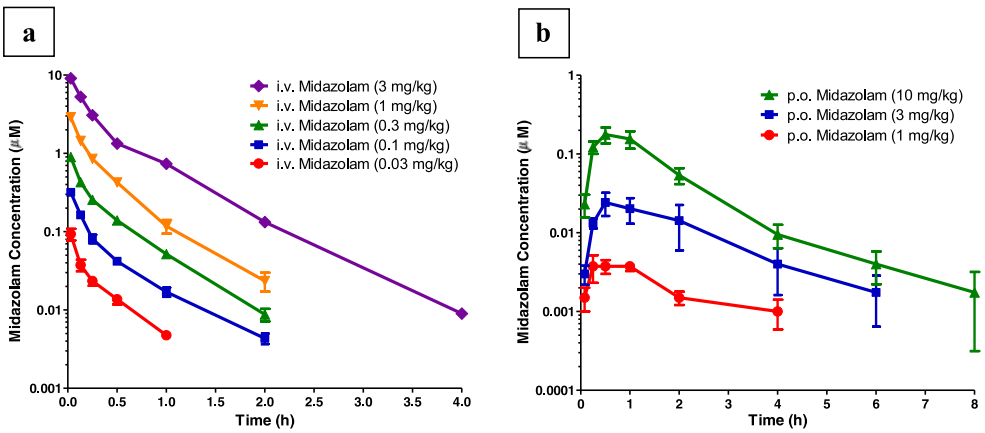

Fig. 5 Plasma PK in male Wistar Hannover rats following either (**A**) intravenous administration of midazolam at 0.03, 0.1, 0.3, 1, and 3 mg/kg dose levels, or (**B**) oral administration of midazolam at 1, 3, and 10 mg/kg dose levels. Groups were $n = 4$ animals and data are expressed as mean ± S.E.M.

Table II Summary of PK Parameters Calculated for Several Doses of Midazolam. Groups were $n = 4$ Rats and Data are Expressed as Mean ± S.E.M.

Midazolam Dose (Route)	AUC (0-∞) (μM·h)	CL (mL/min/kg)	Cmax (μM)
0.03 mg/kg (i.v.)	0.024 ± 0.003	65.5 ± 7.8	-
0.1 mg/kg (i.v.)	0.088 ± 0.005	58.3 ± 2.8	-
0.3 mg/kg (i.v.)	0.260 ± 0.016	59.5 ± 4.3	-
1 mg/kg (i.v.)	0.798 ± 0.064	66.0 ± 5.3	-
3 mg/kg (i.v.)	2.985 ± 0.108	51.5 ± 2.0	-
1 mg/kg (p.o.)	0.015 ± 0.004	-	0.005 ± 0.001
3 mg/kg (p.o.)	0.059 ± 0.027	-	0.024 ± 0.008
10 mg/kg (p.o.)	0.301 ± 0.050	-	0.185 ± 0.041

A "-" in the CL or C_{max} column denotes that the parameter was not determined.

the PK parameters appear to be driven by altered liver metabolism rather than altered gut metabolism.

DISCUSSION

One of the major advantages of using siRNA to achieve POR knockdown instead of a knockout mouse model is that the POR knockdown is transient rather than permanent. As such, it was important to define the kinetics of POR mRNA and protein knockdown, as well as how the loss of POR protein translated into the loss of POR enzyme activity (Fig. 2). siRNA-mediated knockdown of POR mRNA was extremely rapid, with maximum knockdown occurring within 24 h post-dose. In contrast, the POR protein levels took much longer to drop, only reaching maximum knockdown approximately 1 week post-dose. The rate of new POR protein production was drastically reduced as early as 24 h post-dose, but the pre-existing protein takes a week or more to be degraded and lost from the tissue; thus, the pre-existing POR protein seems to have a relatively long half-life in this system where the ability to produce new POR protein has been compromised. Due to the low level of POR protein synthesis that continues (still approximately 10% of POR transcript remains), the 84% protein reduction appears to be the maximal reduction in protein levels that can be achieved. The mRNA expression shows a trend towards rebounding to baseline by 2 weeks post-dose, so the expectation is that the protein levels will also begin to rebound after 2 weeks due to the production of new protein. The fact that maximum loss of POR enzyme activity occurred 2 weeks post-dose guided the use of that timing in all of the subsequent studies.

The impact of POR knockdown on CYP-mediated metabolism in rat liver was first assessed by fitting *in vitro* microsomal stability experiments to Michealis-Menten kinetics (Fig. 3). For commercial rat liver microsomes, the formation of 4-hydroxydiclofenac had a K_m of 13.5 μM and a V_{max} of 1707 pmol/min/mg protein, which are in agreement with literature values reported (K_m of 14 μM and V_{max} of 1400 pmol/min/mg protein) for the 4-hydroxylation of diclofenac in rat liver microsomes (19). While the treated rat liver microsomes with lower POR enzyme activity had a similar K_m of 11.7 μM for the formation of 4-hydroxydiclofenac, the V_{max} was found to be significantly reduced to only 527 pmol/min/mg protein. The functional implication of this result is that POR knockdown did not alter the way the CYP enzyme binds to diclofenac prior to the hydroxylation reaction (K_m), but rather the POR knockdown reduced the rate of metabolite formation once the substrate was bound to the enzyme (V_{max}). It is known from eq. 2 that a reduction in V_{max} would either come from a reduction in k_{cat} or $[E]_0$, or both. The enzyme responsible for metabolism of diclofenac into 4-hydroxydiclofenac in rat liver microsomes is CYP2C6 (20), which has constant mRNA levels up to 7 days after POR knockdown and at 14 days post-dose the CYP2C6 mRNA levels were upregulated approximately 2-fold (data not shown). When the POR knockout mice were examined, it was noted that loss of POR caused an approximately 5-fold increase in the total CYP content in the liver, with evidence of upregulation of several CYP subfamilies including 2C (4, 5).

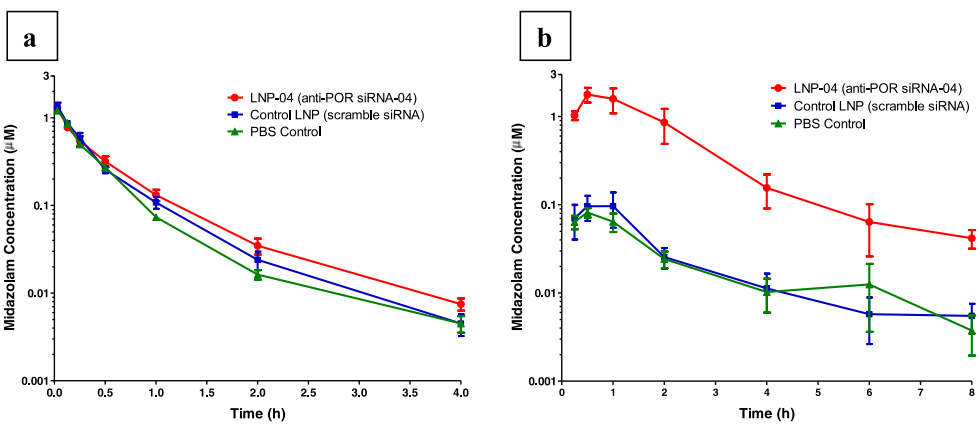

Fig. 6 Plasma PK in male Wistar Hannover rats that received pretreatment with PBS or LNPs 2 weeks prior to dosing midazolam either (**A**) intravenously at 0.5 mg/kg or (**B**) orally at 10 mg/kg. The pretreatment was an i.v. dose of PBS vehicle or LNP containing 1 mg/kg siRNA (either anti-POR siRNA-04 or scrambled siRNA). Groups were $n = 4$ animals and data are expressed as mean ± S.E.M.

Table III Summary of Plasma PK Parameters Calculated for Administration of Midazolam to Rats that Received Various Pretreatments 2 weeks Prior to Midazolam Dosing. Groups were $n = 4$ Rats and Data are Expressed as Mean ± S.E.M.

Midazolam Dose (Route)	siRNA Treatment	AUC (0-∞) (μM·h)	CL (mL/min/kg)	Cmax (μM)
0.5 mg/kg (i.v.)	siRNA-04 (anti-POR)	0.68 ± 0.07	38.5 ± 3.8	-
	scramble siRNA	0.57 ± 0.03	45.3 ± 2.4	-
	PBS (no siRNA)	0.49 ± 0.01	52.0 ± 1.2	-
10 mg/kg (p.o.)	siRNA-04 (anti-POR)	3.85 ± 1.12	-	1.85 ± 0.40
	scramble siRNA	0.22 ± 0.08	-	0.11 ± 0.04
	PBS (no siRNA)	0.19 ± 0.05	-	0.09 ± 0.01

A "-" in the CL or C_{max} column denotes that the parameter was not determined.

So, although the timing of CYP2C6 protein upregulation is unclear, it is likely that $[E]_0$ (*i.e.* the concentration of the CYP2C6 enzyme responsible for diclofenac metabolism) either stays constant or increases. Thus, it is most probable that the decrease in V_{max} is caused by a reduction in the catalytic rate of reaction mediated by the CYP2C6 enzyme (k_{cat}), likely due to the loss of electrons that are normally supplied by POR and are required for the hydroxylation reactions catalyzed by CYPs.

The impact of POR knockdown on CYP-mediated metabolism in rat liver was further assessed by measuring the apparent intrinsic clearance of diclofenac and midazolam in rat liver microsomes (Fig. 4). The $CL_{int,app}$ for diclofenac was determined to be 1,428 mL/min/kg for microsomes from rats treated with PBS and 276 mL/min/kg for microsomes from rats treated with LNP-04 containing anti-POR siRNA-04, representing a 5-fold decrease in the apparent intrinsic clearance of diclofenac following POR knockdown. This decrease in the intrinsic clearance of diclofenac correlates well with the 3-fold reduction in V_{max} for 4-hydroxydiclofenac formation, showing that diclofenac metabolism is significantly reduced due to the loss of POR. The difference in the magnitude of the changes could be due to the use of two different microsome preparations, or it could result from the fact that other metabolites (besides 4-hydroxydiclofenac) can be formed during the clearance measurements. The $CL_{int,app}$ for midazolam was determined to be 3,551 mL/min/kg for microsomes from rats treated with PBS and 406 mL/min/kg for microsomes from rats treated with LNP-04 containing anti-POR siRNA-04, representing a nearly 9-fold decrease in the apparent intrinsic clearance of midazolam following POR knockdown. Similar microsomal stability experiments were conducted with verapamil and bufuralol, with POR knockdown also reducing the metabolism of these substrates (data not shown). Since it is known that the enzyme families mainly responsible for drug metabolism in rats are CYP3A for midazolam, CYP2C for diclofenac, CYP2D for bufuralol, and CYP3A for verapamil (20, 21), it is clear that knockdown of POR has reduced CYP-mediated metabolism across multiple CYP families. Coupled with the fact that Riddick and coworkers have shown reduced metabolism in POR knockout mice using additional probe substrates (6), there is significant evidence that siRNA-mediated knockdown of POR can reduce the clearance of many different compounds that are metabolized by various CYPs, which is an important feature that will enable broad application of this tool to drug discovery and development. Lastly, midazolam was selected for use in the following *in vivo* studies because it was shown to have the highest intrinsic clearance and the largest reduction in intrinsic clearance following POR knockdown.

To understand how the reduced midazolam intrinsic clearance measured *in vitro* following POR knockdown would impact PK parameters *in vivo*, midazolam was dosed i.v. and p.o. 2 weeks after administration of LNPs or PBS. The key findings from these studies were that POR knockdown leads to a 25% decrease in plasma clearance that drives a less than 2-fold increase in the plasma AUC following i.v. administration of midazolam, while POR knockdown leads to a 14-fold increase in bioavailability that drives a 20-fold increase in plasma AUC following p.o. administration of midazolam. Kotegawa and coworkers used ketoconazole (a known inhibitor of CYP3A enzymes that metabolize midazolam) predosed in rats to show that inhibition of metabolism only produced a 30% reduction in plasma clearance following i.v. dose of midazolam, but a nearly 7-fold increase in plasma AUC following p.o. dose of midazolam (22). Although the changes noted in that work differ slightly in magnitude from the changes presented in this work (potentially due to differences in midazolam doses between the studies or differences in the extent of metabolism inhibition by ketoconazole compared to POR knockdown), both studies highlight an overall trend of a larger impact on oral AUC compared to i.v. AUC following inhibition of midazolam metabolism.

The large difference in response to POR knockdown depending on the route of administration for midazolam was explored using two models (the well-stirred model and the parallel tube model) to describe the hepatic extraction of midazolam (Supplementary Material). The overall trends

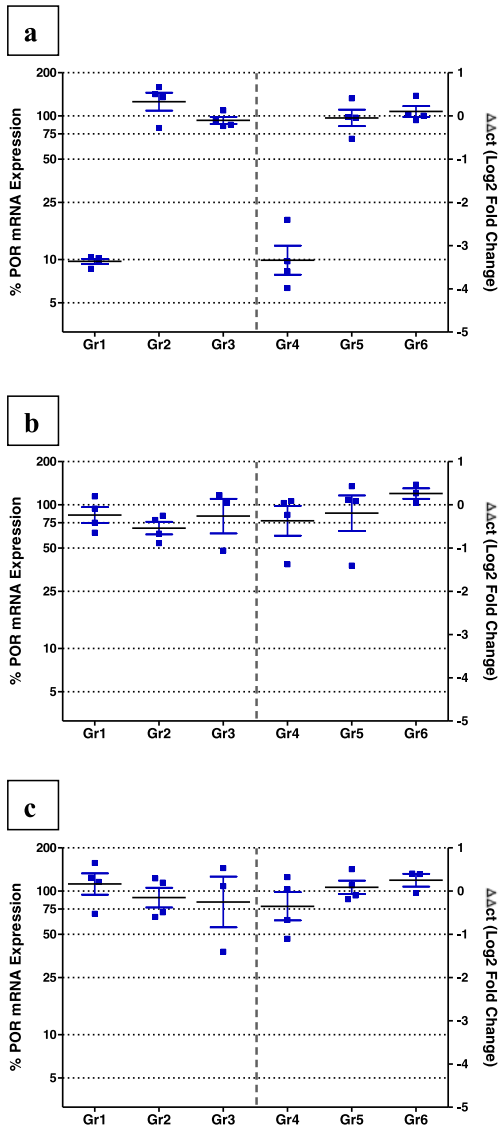

Fig. 7 mRNA knockdown in (**A**) liver, (**B**) duodenum, (**C**) jejunum 15 days after a 1 mg/kg dose of LNP-04, control LNP, or PBS. Groups are as follows: Gr1 and Gr4 are LNP-04 (anti-POR siRNA-04); Gr2 and Gr5 are control LNP (scrambled siRNA); Gr3 and Gr6 are PBS control. Groups 1–3 received midazolam by i.v. route, while groups 4–6 received midazolam *via* p.o. route. POR mRNA levels are normalized to mRNA levels of the housekeeping gene Ppib and all data are normalized relative to 100% expression for PBS control group. Groups were $n = 4$ animals and data are expressed as mean ± S.E.M.

from the data are predicted by the parallel tube model: POR knockdown decreases CYP-mediated metabolism thus reducing the unbound intrinsic clearance ($CL_{int,u}$), which leads to a reduction in hepatic extraction ratio (ER_H) and an increase in the fraction of drug that passes through the liver without being metabolized (F_H). The increase in F_H drives only small reductions in blood clearance following an i.v. dose of midazolam, but generates large increases in oral bioavailability and blood AUC following a p.o. dose of midazolam (Supplementary Material). The blood AUC of midazolam following an i.v. dose is inversely proportional to blood clearance (CL_b), and CL_b is assumed to be equal to hepatic blood clearance ($CL_{b,h}$) because the vast majority of midazolam blood clearance is due to metabolism in the liver. The parallel tube model was used to describe $CL_{b,h}$ as a function of $CL_{int,u}$ (eq. 15 in the Supplementary Material) and it can be seen from this relationship that $CL_{b,h}$ asymptotically approaches liver blood flow with increasing $CL_{int,u}$ (Fig. 8A). In this case, the $CL_{b,h}$ values derived from the model (red squares in Fig. 8a and Table V in the Supplementary Material) predict a larger difference in CL_b from rats with and without POR knockdown than what was actually measured *in vivo*. One explanation for the discrepancy could potentially be that the $CL_{int,u}$ measured *in vitro* underestimates the true $CL_{int,u}$ *in vivo*, with higher values of $CL_{int,u}$ producing smaller differences in $CL_{b,h}$ between rats with and without POR knockdown (eq. 16 in the Supplementary Material). Consequently, POR knockdown will cause only small changes in blood AUC following i.v. dosing for high $CL_{int,u}$ compounds like midazolam. The parallel tube model was used to describe the bioavailability (F) of midazolam following an oral dose as a function of $CL_{int,u}$ (eq. 17 in the Supplementary Material) and it can be seen from this relationship that F asymptotically approaches zero with increasing $CL_{int,u}$ (Fig. 8B). In this case, the F values derived from the model (red squares in Fig. 8B and Table V in the Supplementary Material) predict higher overall values and a smaller difference in F from rats with and without POR knockdown than what was actually measured *in vivo*. Again assuming that $CL_{int,u}$ was underestimated *in vitro*, it can be seen that higher values of $CL_{int,u}$ would produce lower overall F values as well as larger differences between rats with and without POR knockdown (eq. 18 in the Supplementary Material). In fact, as $CL_{int,u}$ increases, the ratio of the bioavailability in rats with POR knockdown to the bioavailability in PBS-treated rats exponentially increases. Accordingly, POR knockdown will cause large changes in blood AUC following p.o. dosing for high $CL_{int,u}$ compounds like midazolam. Thus, siRNA-mediated knockdown of POR should be very useful as a tool applied during drug discovery and development to increase exposure following p.o. administration of unoptimized compounds with high intrinsic clearances due to CYP-mediated metabolism in the liver.

Finally, this work was initiated based on the critical role that POR plays in donating electrons to CYP enzymes to mediate drug metabolism. The mechanism of CYP-mediated oxidation requires the sequential transfer of two electrons and then two protons to coordinate the iron and oxygen of the heme group into the oxyferryl intermediate that is capable of oxygenating the substrate (23). POR is able to transfer the first and second electrons from NADPH to the heme group of the CYP, but it has been commonly accepted that cytochrome b_5 is only capable of transferring the second (rate-limiting) electron. In recent work, CYP2B4 was stoichiometrically reduced by dithionite to mimic the effect of

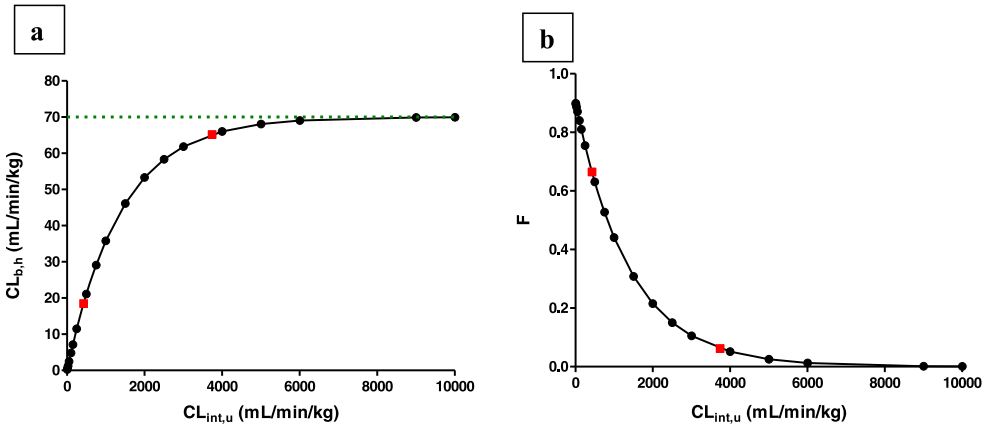

Fig. 8 Utilizing the parallel tube liver model, (**A**) hepatic blood clearance ($CL_{b,h}$) and (**B**) bioavailability (F) of midazolam were calculated as a function of unbound intrinsic clearance ($CL_{int,u}$) using the parameter values and equations presented in the Supplementary Material. The red squares mark the unbound intrinsic clearance values determined for midazolam in liver microsomes from PBS treated rats ($CL_{int,u}$ = 3738 mL/min/kg) and rats with POR knockdown ($CL_{int,u}$ = 427 mL/min/kg). In part (**A**), a dotted line was drawn at the point where hepatic blood clearance equals liver blood flow ($CL_{b,h} = Q_H$ = 70 mL/min/kg). In part (**B**), the maximum value for F is approximately 0.9 due to the assumption that F_A and F_G both equal 0.95 as discussed in the Supplementary Material.

transferring the first electron, and then cytochrome b_5 was shown to mediate catalysis of substrate oxidation by CYP2B4 at a rate that was 10- to 100-fold faster than POR (24). To explore the *in vivo* role of cytochrome b_5 in the function of CYPs, Finn *et al.* created a conditional knockout mouse with hepatic deletion of cytochrome b_5 using an Alb-Cre/loxP system similar to the one discussed above for the POR knockout mouse (25). Liver microsomes produced from the knockout mice showed reduced V_{max} for metabolism of several substrates and administration of these substrates (including midazolam) *in vivo* revealed slower clearance and higher plasma concentrations due to reduced metabolism following cytochrome b_5 deletion in the liver (25). Knockout mice with conditional deletion of cytochrome b_5 developed normally, with no alterations in liver morphology, hepatic lipid content, or liver function biomarkers (25). In addition, knockout mice with complete deletion of cytochrome b_5 in all tissues were created and shown to be viable, fertile, and exhibiting no gross anatomical abnormalities (26), in contrast to the complete deletion of POR that was embryonic lethal (3). The hepatic POR conditional knockout mouse line was crossed with the hepatic cytochrome b_5 conditional knockout mouse line to produce conditional double knockout mice lacking both hepatic POR and cytochrome b_5, and it was shown that these mice were viable, fertile, and exhibited no gross anatomic abnormalities (27). The authors used microsomes from the POR single knockout mice to show that cytochrome b_5 (together with cytochrome b_5 reductase) was the source of electrons in the absence of POR, providing evidence that cytochrome b_5 can act as the sole electron donor to CYPs in certain circumstances (27). The functional output of this result is that the loss of both cytochrome b_5 and POR would have a synergistic effect on the reduction of CYP-mediated drug metabolism, and it was shown that midazolam had a large increase in oral plasma AUC in the double knockout mice compared to both types of single knockout mice (27). However, the downside to using the double knockout mice is the large increase in hepatic lipid accumulation that leads to extensive vacuolation typical of steatotic liver (27), so again the use of siRNA to achieve the knockdown of both cytochrome b_5 and POR in a transient manner provides a dramatic benefit. Development of the tool using double siRNA-mediated knockdown of both POR and cytochrome b_5 to increase drug exposure is ongoing in our labs, and in the future will be applied to drug discovery programs to show the utility of generating faster lead identification and target validation.

CONCLUSION

siRNAs were designed against POR and LNPs were used to deliver the siRNAs *in vivo*. In male Wistar Hannover rats, the anti-POR siRNA was shown to generate ~90% POR mRNA knockdown, ~85% POR protein knockdown, and ~85% reduction in POR enzyme activity out to 2 weeks post-dose. The *in vitro* microsomal metabolism experiments showed that POR knockdown significantly reduced the metabolic clearance of diclofenac, midazolam, verapamil, and bufuralol, which are metabolized by several different families of CYP enzymes. *In vivo*, LNPs with anti-POR siRNAs were administered and then followed by i.v. or p.o. doses of midazolam 2 weeks later, where knockdown of POR manifested as reduced clearance, higher bioavailability, and higher plasma concentrations of midazolam. Consistent with the fact that midazolam is a high clearance compound, the magnitude of the impact on the PK parameters was much greater following p.o. administration of midazolam compared to i.v.

administration. The parallel tube liver model was shown to closely predict the observed effects following POR knockdown, including the trends of a smaller impact on i.v. clearance and a larger impact on oral bioavailability. This work clearly demonstrates that siRNA can be used as a tool to increase the *in vivo* exposure of orally administered midazolam and should be generalizable for all high clearance compounds that are predominantly metabolized by CYP enzymes in the liver.

ACKNOWLEDGMENTS AND DISCOLSURES

The authors would like to thank Matthew Shipton and Carolyn Six at BioreclamationIVT for their assistance with the production of custom liver and intestinal microsomes from the treated and control rats. All authors were employed by Merck & Co., Inc. at the time this research was performed.

REFERENCES

1. Strelevitz TJ, Foti RS, Fisher MB. *In vivo* use of the P450 inactivator 1-aminobenzotriazole in the rat: varied dosing route to elucidate gut and liver contributions to first-pass and systemic clearance. J Pharm Sci. 2006;95:1334–41.
2. Linder CD, Renaud NA, Hutzler JM. Is 1-aminobenzotriazole an appropriate *in vitro* tool as a nonspecific cytochrome P450 inactivator? Drug Metab Dispos. 2009;37:10–3.
3. Shen AL, O'Leary KA, Kasper CB. Association of multiple developmental defects and embryonic lethality with loss of microsomal NADPH-cytochrome P450 oxidoreductase. J of biol chem. 2002;277:6536–41.
4. Gu J, Weng Y, Zhang QY, Cui H, Behr M, Wu L, *et al.* Liver-specific deletion of the NADPH-cytochrome P450 reductase gene: impact on plasma cholesterol homeostasis and the function and regulation of microsomal cytochrome P450 and heme oxygenase. J of biol chem. 2003;278:25895–901.
5. Henderson CJ, Otto DME, Carrie D, Magnuson MA, McLaren AW, Rosewell I, *et al.* Inactivation of the hepatic cytochrome P450 system by conditional deletion of hepatic cytochrome P450 reductase. J Biol Chem. 2003;278:13480–6.
6. Riddick DS, Ding XX, Wolf CR, Porter TD, Pandey AV, Zhang QY, *et al.* NADPH-cytochrome P450 oxidoreductase: roles in physiology, pharmacology, and toxicology. Drug Metab Dispos. 2013;41:12–23.
7. Akinc A, Querbes W, De SM, Qin J, Frank-Kamenetsky M, Jayaprakash KN, *et al.* Targeted delivery of RNAi therapeutics with endogenous and exogenous ligand-based mechanisms. Mol Ther. 2010;18:1357–64.
8. Semple SC, Akinc A, Chen JX, Sandhu AP, Mui BL, Cho CK, *et al.* Rational design of cationic lipids for siRNA delivery. Nat Biotechnol. 2010;28:172–U118.
9. Jayaraman M, Ansell SM, Mui BL, Tam YK, Chen JX, Du XY, *et al.* Maximizing the potency of siRNA lipid nanoparticles for hepatic gene silencing *In vivo*. Angew Chem Int Ed. 2012;51:8529–33.
10. Maier MA, Jayaraman M, Matsuda S, Liu J, Barros S, Querbes W, *et al.* Biodegradable lipids enabling rapidly eliminated lipid nanoparticles for systemic delivery of RNAi therapeutics. Mol Ther. 2013;21:1570–8.
11. Coelho T, Adams D, Silva A, Lozeron P, Hawkins PN, Mant T, *et al.* Safety and efficacy of RNAi therapy for transthyretin amyloidosis. N Engl J Med. 2013;369:819–29.
12. Wincott F, Direnzo A, Shaffer C, Grimm S, Tracz D, Workman C, *et al.* Synthesis, deprotection. Anal Purif Rna Ribozymes Nucleic Acids Res. 1995;23:2677–84.
13. M. Tadin-Strapps, L.B. Peterson, A.M. Cumiskey, R.L. Rosa, V.H. Mendoza, J. Castro-Perez, O. Puig, L.W. Zhang, W.R. Strapps, S. Yendluri, L. Andrews, V. Pickering, J. Rice, L. Luo, Z. Chen, S. Tep, B. Ason, E.P. Somers, A.B.. Sachs, S.R. Bartz, J. Tian, J. Chin, B.K. Hubbard, K.K. Wong, and L.J. Mitnaul. siRNA-induced liver ApoB knockdown lowers serum LDL-cholesterol in a mouse model with human-like serum lipids. Journal of Lipid Research. 52:1084-1097 (2011).
14. Gindy ME, Leone AM, Cunningham JJ. Challenges in the pharmaceutical development of lipid-based short interfering ribonucleic acid therapeutics. Expert Opin on Drug Deliv. 2012;9:171–82.
15. A. Walser, L.E. Benjamin, T. Flynn, C. Mason, R. Schwartz, and R.I. Fryer. Quinazolines and 1,4-Benzodiazepines .84. Synthesis and Reactions of Imidazo [1,5-a] [1,4] Benzodiazepines. Journal of Organic Chemistry. 43:936-944 (1978).
16. A. Walser and R.I. Fryer. Quinazolines and 1,4-Benzodiazepines .93. Synthesis of Imidazo [1,5-a] [1,4] Benzodiazepines from Nitrooximes. Journal of Heterocyclic Chemistry. 20:551-558 (1983).
17. Obach RS, Baxter JG, Liston TE, Silber BM, Jones BC, MacIntyre F, *et al.* The prediction of human pharmacokinetic parameters from preclinical and *in vitro* metabolism data. J Pharmacol Exp Ther. 1997;283:46–58.
18. Obach RS. Prediction of human clearance of twenty-nine drugs from hepatic microsomal intrinsic clearance data: an examination of *in vitro* half-life approach and nonspecific binding to microsomes. Drug Metab Dispos. 1999;27:1350–9.
19. Kumar S, Samuel K, Subramanian R, Braun MP, Stearns RA, Chiu SHL, *et al.* Extrapolation of diclofenac clearance from *in vitro* microsomal metabolism data: Role of acyl glucuronidation and sequential oxidative metabolism of the acyl glucuronide. J Pharmacol Exp Ther. 2002;303:969–78.
20. Kobayashi K, Urashima K, Shimada N, Chiba K. Substrate specificity for rat cytochrome P450 (CYP) isoforms: screening with cDNA-expressed systems of the rat. Biochem Pharmacol. 2002;63:889–96.
21. Choi JS, Burm JP. Effect of pioglitazone on the pharmacokinetics of verapamil and its major metabolite, norverapamil, in rats. Arch Pharm Res. 2008;31:1200–4.
22. Kotegawa T, Laurijssens BE, Von Moltke LL, Cotreau MM, Perloff MD, Venkatakrishnan K, *et al. In vitro*, pharmacokinetic, and pharmacodynamic interactions of ketoconazole and midazolam in the rat. J pharmacol exp ther. 2002;302:1228–37.
23. Denisov IG, Makris TM, Sligar SG, Schlichting I. Structure and chemistry of cytochrome P450. Chem Rev. 2005;105:2253–77.
24. Zhang HM, Im SC, Waskell L. Cytochrome b (5) increases the rate of product formation by cytochrome p450 2B4 and competes with cytochrome p450 reductase for a binding site on cytochrome p450 2B4. J Biol Chem. 2007;282:29766–76.
25. Finn RD, McLaughlin LA, Ronseaux S, Rosewell I, Houston JB, Henderson CJ, *et al.* Defining the *in vivo* role for cytochrome b (5) in cytochrome P450 function through the conditional hepatic deletion of microsomal cytochrome b (5). J Biol Chem. 2008;283:31385–93.
26. McLaughlin LA, Ronseaux S, Finn RD, Henderson CJ, Wolf CR. Deletion of microsomal cytochrome b (5) profoundly affects hepatic and extrahepatic drug metabolism. Mol Pharmacol. 2010;78:269–78.
27. Henderson CJ, McLaughlin LA, Wolf CR. Evidence that cytochrome b_5 and cytochrome b_5 reductase Can Act as sole electron donors to the hepatic cytochrome P450 system. Mol Pharmacol. 2013;83:1209–17.